An atom faucet

W. Wohlleben[a], F. Chevy, K. Madison, and J. Dalibard[b]

Laboratoire Kastler Brossel[c], Département de Physique de l'École Normale Supérieure, 24 rue Lhomond,
75005 Paris, France

Abstract. We present a simple and efficient source of slow atoms. From a background vapour loaded magneto-optical trap (MOT), a thin laser beam extracts a continuous jet of cold rubidium atoms. The jet that is typical to leaking MOT systems is created without any optical parts placed inside the vacuum chamber. We also present a simple three dimensional numerical simulation of the atomic motion in the presence of these multiple saturating laser fields combined with the inhomogeneous magnetic field of the MOT. At a pressure of $P_{\mathrm{Rb87}} = 10^{-8}$ mbar and with a moderate laser power of 10 mW per beam, we generate a flux $\Phi = 1.3 \times 10^8$ atoms/s with a mean velocity of 14 m/s and a divergence of 10 mrad.

PACS. 32.80.Lg Mechanical effects of light on atoms, molecules, and ions – 32.80.Pj Optical cooling of atoms; trapping

1 Introduction

Experiments on trapped, cold atoms require in most cases high particle numbers and long trapping lifetimes. In order to restrict the collisions with background gas which limit the lifetime, an ultra-high vacuum (UHV) environment is necessary. In turn, at these low pressures, a very long time (which can reach several minutes) is required to load a magneto-optical trap (MOT) from the background vapour pressure. To circumvent this problem, an additional jet of cold atoms is commonly employed to load the trap. The simplest possible cold atom source consists in a velocity filter [1], but the flux is then quite low. It can be greatly improved by adding a laser cooling stage, such as a Zeeman slower which is widely used especially for light and thus thermally non capturable species. For heavier elements, an attractive alternative consists in accumulating atoms into a MOT in an auxiliary vapour cell, with various strategies for subsequent transfer to a recapture MOT in the UHV cell. These strategies can be categorized into either a pulsed [2–4] or continuous transfer scheme. The latter category involves either a moving molasses [5] or a "leaking MOT" scheme [6–8].

This paper presents the construction and the numerical modeling of a cold atom jet whose flux is continuous, adjustable in a given direction, and velocity tunable. The device is based on a vapour charged MOT

(VCMOT) located in a glass cell with a rubidium pressure of $P \sim 10^{-8}$ mbar. It captures and cools atoms from the low velocity part of the Maxwell-Boltzmann distribution at room temperature. A push beam of ~ 1 mm spot size is focused at the center of this source MOT. It extracts a continuous jet that is slow enough to be recaptured in a MOT located in the UHV region. The jet passes through a tube that maintains the pressure differential between the two cells, and the transfer efficiency between the two MOTs is found to be typically 50%.

The atom faucet is closely related to the low velocity intense source (LVIS) [6], the bi-dimensional magneto optical trap (2D$^+$MOT) [7] and the pyramidal funnel [8]. The common concept which relates them in the "leaking MOT" family is the creation of a thin extraction column in the center of the MOT. In this column the radiation pressure is imbalanced, which generates a continuous jet of cold atoms. Operation in a continuous mode maximizes the mean flux up to a value ideally equal to the source trap capture rate. Since a leaking trap operates at a low trap density, once captured, an atom has much higher probability to leave the trap *via* the jet rather than undergoing a collision with another trapped atom that would expel it. The pyramidal funnel [8] is constituted by a single pyramidal mirror [9] with a hole at its tip. The LVIS and 2D$^+$MOT in [6] and [7] place a plane mirror inside the vacuum for retroreflection of one of the MOT beams. By piercing a hole in the retroreflection mirror, one creates a hollow retroreflection beam, and the jet exits through the hole. By contrast, the atom faucet requires no optical parts inside the vacuum system. Here, we superimpose an additional collimated "push beam" that pierces the extraction column through the MOT.

---

[a] *Present address:* Max-Planck-Institut für Quantenoptik, 85748 Garching, Germany.
[b] e-mail: `jean.dalibard@lkb.ens.fr`
[c] Unité de Recherche de l'École normale supérieure et de l'université Pierre et Marie Curie, associée au CNRS.

In these complex magneto-optical arrangements the behavior of the system is no longer intuitive. On its way into the jet, a thermal atom undergoes subsequent phases of strong 3D radiation pressure (capture from vapour), overdamped guidance to the magnetic field minimum, and 1D strong radiation pressure with transverse 2D cooling (extraction process). Usually, theoretical estimates for near-resonant atom traps concentrate either on the capture [10] or on the cooling [11]. Here we develop a simple and heuristic generalization of the expression of the semi-classical radiation pressure force in the case of multiple saturating laser fields and in presence of an inhomogeneous magnetic field. We integrate the equation of motion of the atoms as they undergo the capture and the cooling processes. Our results reproduce well the parameter dependences of the atom faucet found experimentally. However, the fact that we neglect optical pumping and particle interaction, associated with the simplifications made to the rubidium level scheme, lead to an overestimation of the absolute value of the radiation pressure force and hence to an overestimate for the capture velocity of the MOT.

This paper is organized as follows. In Section 2 we detail the experimental realization of the atom faucet. In Section 3 we present our theoretical model. Section 4 discusses the parameter dependences of the device in the experiment and in the simulations. Finally in Section 5 we compare this scheme to other vapour cell cold atom sources.

2 Experimental realisation

The vacuum system consists of two glass cells separated vertically by 67 cm with a MOT aligned at the center of each cell. A heated reservoir connected to the upper source cell supplies the rubidium vapour. The ^{87}Rb pressure (typically 10^{-8} mbar) in this source cell is measured from the resonant absorption of a probe beam. Using an appropriate pumping scheme and a differential pumping tube of diameter 5 mm and length 15 cm, the pressure in the lower recapture cell is maintained to a value below 10^{-11} mbar.

The atom faucet (see Fig. 1) is based on a standard MOT configuration: two anti-Helmholtz-coils maintain a magnetic field gradient of 15 G/cm along their axis, which is horizontal in this setup. The laser system is realized by a grating stabilized diode laser locked to the $|5S_{1/2}, F = 2\rangle \rightarrow |5P_{3/2}, F = 3\rangle$ transition. It injects into three slave lasers, two for the source MOT and one for the recapture MOT.

For the source MOT, a pair of counterpropagating laser beams with positive helicity is aligned with the axis of the coils (axial beams); two mutually orthogonal pairs of counterpropagating beams with negative helicity are located in the symmetry plane of the coils. These radial beams are inclined by 45° with respect to the vertical direction. The axial (radial) trap beam(s) have an 11 (8) mm spot size, all clipped to a diameter of 24 mm by the quarter wave plate mounts. The power of the axial (radial)
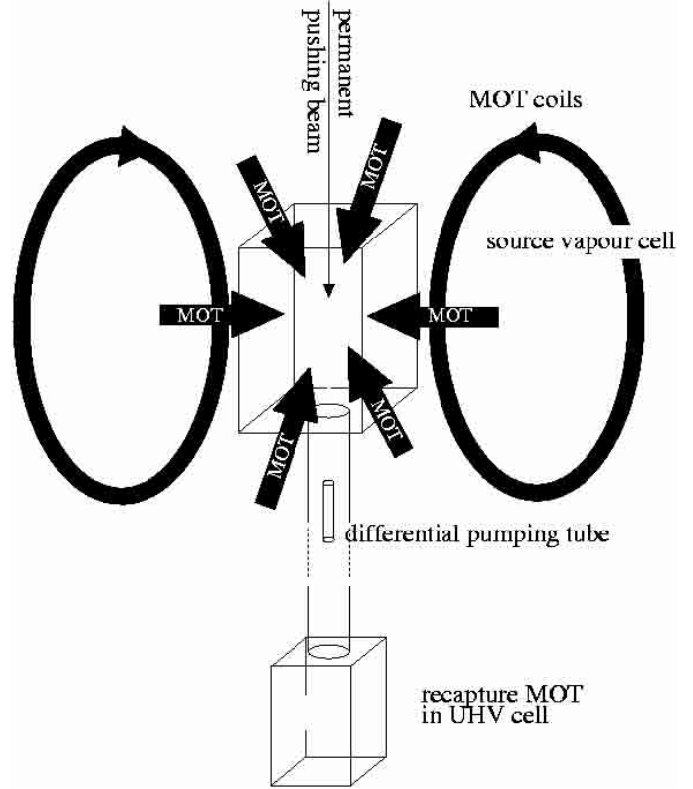

Fig. 1. The atom faucet setup (with the recapture MOT below). A permanent push beam with ~ 1 mm spot size creates an extraction column from an ordinary vapour charged MOT. The upper high pressure region is separated from the ultra-high-vacuum region by a differential pumping tube. The pressure in the source cell is monitored by the absorption of an additional probe beam (not shown).

beam(s) is 20 mW (5 mW) before retroreflection. To prevent optical pumping into the $|5S_{1/2}, F = 1\rangle$ hyperfine ground level, a repumping laser beam, resonant with the $|5S_{1/2}, F = 1\rangle \rightarrow |5P_{3/2}, F = 2\rangle$ transition, is mixed with the axial trapping beam. It is provided by an independent grating stabilized laser and it has a power of 5 mW.

In addition to these trapping and repumping beams, a permanent push beam is aligned vertically and centered onto the trap. The push beam is quasi resonant with the $|5S_{1/2}, F = 2\rangle \rightarrow |5P_{3/2}, F = 3\rangle$ transition; it has a linear polarization [13] and a typical power of 200 μW. The detailed variations of the atom faucet behaviour with the detuning and the power of the push beam are given below (Sect. 4). It is focused to a waist of 90 μm with the focal spot located 30 cm before entering the source cell. This push beam thus diverges to a size of 1.1 mm at the source trap and 3.3 mm at the recapture trap. Its intensity at the center of the source MOT is comparable to those of the MOT beams. Hence it creates a radiation pressure force comparable with the trapping forces in the MOT. Because of its divergence, the push beam has an intensity in the lower MOT lower by a factor 10 than in the upper MOT. Therefore it decenters the recapture MOT
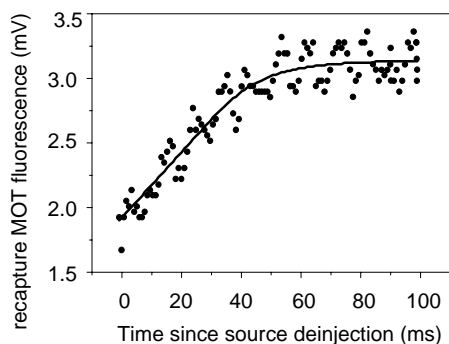
Fig. 2. (•) Temporal variation of the fluorescence of the atoms confined in the recapture trap after sudden disinjection of the source MOT beams. The push beam is not changed in order to keep constant its influence on the lower trap fluorescence. The fit (solid line) is made assuming a velocity distribution $\Phi(v) = \Phi_0 \exp\left(-(v - \bar{v})^2/2\delta v^2\right)$ and it yields $\bar{v} = 14$ m/s and $\delta v = 9$ m/s.

by ~ 1 mm but does not destabilize it. The push beam carries no repumping light, so that it pumps the atoms in the $|5S_{1/2}, F = 1\rangle$ hyperfine sublevel and it acts on the atoms only where it intersects the upper or lower MOT beams, in which repumping light is present.

By studying the loading characteristics of the recapture MOT, we deduce the main features of the atom jet. In particular, we investigate two features of the loading process.

1. When the recapture MOT is empty, the initial recapture rate gives directly the recaptured flux since the density dependent intrinsic losses in the MOT are not yet important. The absolute number of atoms is determined using an absorption imaging technique.

2. The time dependence of the recapture rate provides a measurement of the longitudinal velocity distribution of the jet. More precisely, by suddenly disinjecting the source MOT slave lasers and then recording the recapture loading rate via the fluorescence, the characteristics of the tail of the moving extraction column are measured. The jet transfer distance $D = 67$ cm and the time delay T of the loading rate response gives the mean longitudinal velocity $\bar{v} = D/T$ in the jet, and the time width Δt of this response gives access to the longitudinal velocity dispersion δv (see Fig. 2).

The transfer efficiency is deduced from the loading rate of the source MOT, determined by its fluorescence, in comparison with the measured recapture rate. The fluorescence measurement is done by switching rapidly the MOT beams at resonance and by monitoring the maximum of the signal emitted by the trapped atoms, before they escape from the trap. We assume full saturation of the transition under the influence of all six laser beams and thus a photon scattering rate of $\Gamma/2$ photons/atom.

We observe a typical transfer efficiency of 50% (see below). Assuming for the moment the atom jet divergence to be the only loss contribution, we can interpret the transfer efficiency as a conservative upper limit on the atom

jet divergence. Given the radius of the recapture MOT beams $r = 5$ mm and the transfer distance $D = 67$ cm, at least 50% of the atoms captured into the source MOT are emitted with a divergence better than $r/D \sim 10$ mrad.

3 Numerical model

In order to model both the capture of atoms from the vapour into the source MOT and the subsequent cooling and pushing processes, we have developed a numerical simulation which integrates the equation of motion for atoms chosen with random initial positions and velocities. We describe the atomic motion using classical dynamics. The action of the seven laser beams (6 MOT beams + 1 push beam) on an atom located at $\mathbf{r}$ with velocity $\mathbf{v}$ is taken into account through an average radiation force $\mathbf{F}(\mathbf{r}, \mathbf{v})$. We neglect any heating or diffusion caused by spontaneous emission.

The calculation of the semi-classical force acting on an atom in this multiple beam configuration is *a priori* very complex. For simplicity, we model the atomic transition as a $|g, J_g = 0\rangle \leftrightarrow |e, J_e = 1\rangle$ transition with frequency $\hbar \omega_A$, where $|g\rangle$ and $|e\rangle$ stand for the ground and excited state respectively. We denote Γ^{-1} the lifetime of $|e\rangle$. To motivate the approximate expression that we choose for the radiation pressure force acting on an atom, we shall proceed in several steps. We consider first a single plane-wave beam with wave vector $\mathbf{k}$, detuning $\delta = \omega_L - \omega_A$, intensity I, and polarisation $\sigma_\pm$ along the local magnetic field $\mathbf{B}$ in $\mathbf{r}$. The radiation pressure force [14] reads

$$\mathbf{F} = \hbar \mathbf{k} \, \frac{\Gamma}{2} \, \frac{s(\mathbf{r}, \mathbf{v})}{1 + s(\mathbf{r}, \mathbf{v})} \tag{1}$$

where the saturation parameter is given by

$$s(\mathbf{r}, \mathbf{v}) = \frac{I}{I_{\text{sat}}} \frac{\Gamma^2}{\Gamma^2 + 4(\delta - \mathbf{k} \cdot \mathbf{v} \pm \mu B/\hbar)^2}.$$

μ is the magnetic moment associated with level $|e\rangle$ and I_{sat} is the saturation intensity for the transition ($I_{\text{sat}} = 1.62$ mW/cm^2 for the D_2 resonance line in Rb). Still restricting our attention to a single traveling wave, we consider now the case where the light couples $|g\rangle$ to two or three Zeeman sublevels $|e_m\rangle$. The calculation is in this case more involved since it requires the solution of the optical Bloch equations, which consist in 16 coupled differential equations. A simple approximation is obtained in the low saturation limit ($s \ll 1$):

$$\mathbf{F} = \hbar \mathbf{k} \, \frac{\Gamma}{2} \sum_{m=-1,0,1} s_m(\mathbf{r}, \mathbf{v}) \tag{2}$$

with

$$s_m = \frac{I_m}{I_{\text{sat}}} \frac{\Gamma^2}{\Gamma^2 + 4(\delta - \mathbf{k} \cdot \mathbf{v} + m\mu B/\hbar)^2}$$

and where I_m is the intensity of the laser wave driving the $|g\rangle \leftrightarrow |e_m\rangle$ transition. We can sum up the three forces

associated with the three possible transitions, each calculated with the proper detuning taking into account the Zeeman effect.

Still working in the low intensity limit, we can generalize equation (2) to the case where N laser beams with wave vectors $\mathbf{k}_j$ and detunings δ_j, $(j = 1, ..., N)$ are present. The force then reads

$$\mathbf{F} = \sum_j \hbar\mathbf{k}_j \; \frac{\Gamma}{2} \sum_{m=-1,0,1} s_{j,m}(\mathbf{r},\mathbf{v}) \qquad (3)$$

with

$$s_{j,m} = \frac{I_{j,m}}{I_{\mathrm{sat}}} \; \frac{\Gamma^2}{\Gamma^2 + 4(\delta_j - \mathbf{k}_j \cdot \mathbf{v} + m\mu B/\hbar)^2}.$$

In establishing equation (3) we have taken the spatial average of the radiative force over a cell of size $\lambda = 2\pi/k$, thus neglecting all interference terms varying as $i(\mathbf{k}_j - \mathbf{k}_{j'}) \cdot \mathbf{r}$. We thereby neglect any effect of the dipole force associated with the light intensity gradients on the wavelength scale. This is justified in the case of a leaking MOT since the associated dipole potential wells are much shallower than the expected energy of the atoms before extraction.

At the center of the capture MOT, we can no longer neglect saturation effects since the saturation parameter for each of the 7 beams is $\sim 1/7$. In principle, accounting for this saturation effect requires a step-by-step numerical integration of the 16 coupled Bloch optical equations (for a $|g, J_g = 0\rangle \leftrightarrow |e, J_e = 1\rangle$ transition), as the atom moves in the total electric field resulting from the interference of all the laser beams present in the experiment. Such a calculation is unfortunately much too intensive to lead to interesting predictions in a reasonable time. We therefore turn to an approximate heuristic expression for the force, demanding that it fulfills the three following conditions:

1. in the case of a single traveling wave, $\sigma_\pm$ polarized along the magnetic field, we should recover expression (1);
2. in the low intensity limit, the force should simplify to expression (3);
3. the magnitude of the force should never exceed $\hbar k\Gamma/2$, which is the maximal radiation pressure force in a single plane wave.

There are of course an infinite number of expressions which fulfill these three conditions. We choose the simplest one:

$$\mathbf{F} = \sum_i \hbar\mathbf{k}_i \; \frac{\Gamma}{2} \; \frac{\sum_m s_{i,m}}{1 + \sum_{j,m} s_{j,m}} \qquad (4)$$

with partial saturation parameters $s_{j,m}$ as defined in equation (3). This equation is the generalization of the heuristic expression used by Phillips and co-workers [11] to account for saturation effects in an optical molasses. It is also consistent with equation (25) of [12], written for trapped atoms whose resonance transition involves arbitrary angular momenta. However, the result of [12] only allows to calculate the average fluorescence rate of the atoms and it does not give access to the net force acting on the atoms.
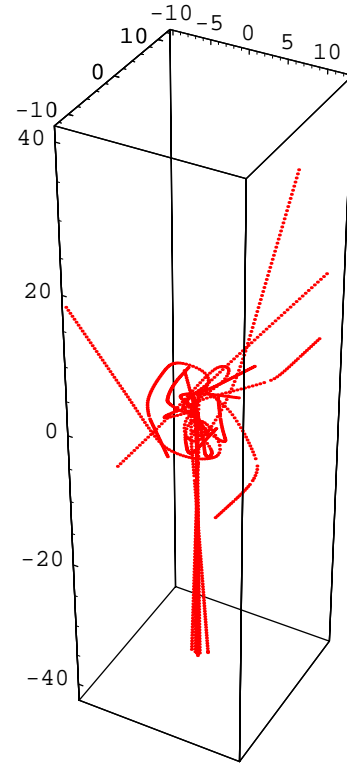

Fig. 3. Some simulated trajectories of atoms in the VCMOT + push beam. The trajectories show how atoms are captured and transfered to the jet (distances in mm).

In our simulation, the MOT beams have a Gaussian profile truncated to the diameter of the quarter wave plate mounts. They all have identical power with an intensity at center equal to $5I_{\mathrm{sat}}$. The intensity of the push beam is of the same order. We assume that because of optical pumping into the lower hyperfine ground state, an atom feels no force when it has left the repumper light mixed into the axial beams. Finally, the magnetic quadrupole field is $\mathbf{B}(\mathbf{x}) = b'(-2x, y, z)$.

In the simulation the initial position of each atom is chosen following a uniform spatial distribution on the cell windows. The initial velocity is given by the Maxwell Boltzmann distribution for $T = 300$ K. The trajectory is then integrated using the Runge-Kutta method. By computing a large number of trajectories such as in Figure 3, one obtains a probability for an atom to be captured and transferred into the jet, as well as the jet characteristics which are the velocity distribution, the divergence, and the total flux. The total flux of the simulated jet is calculated using the real number of atoms $\dot{\mathcal{N}}$ emitted per unit time and per unit surface of the cell at a pressure P: $\dot{\mathcal{N}} = P/\sqrt{2\pi m k_\mathrm{B} T}$ [15,16].

The simulation neglects interaction effects like collisions and multiple light scattering. The validity of the linear scaling with pressure is limited to the low pressure regime $(P < 10^{-7}$ mbar) where the characteristic

extraction time of $\simeq 20$ ms is shorter than the collision time. This collision time is in turn of the order of the trap lifetime measured in absence of push beam.

4 Numerical and experimental results

4.1 The vapour loaded MOT

From the comparison between simulation and experiment, we find that the numerical model overestimates the capture velocity of the MOT, so that we need to calibrate its predictions. Therefore we simulate a pure MOT without push beam and compare the predicted capture rate of

$$\tau_{\text{sim}}^{\text{MOT}} = 13 \times 10^8 \text{ atoms/s} \times P_{\text{Rb87}}(10^{-8} \text{ mbar})$$

with the value we measured in the initial regime of linear growth of the vapour charged source MOT, while the push beam is switched off

$$\tau_{\text{exp}}^{\text{MOT}} = 2.5 \pm 0.6 \times 10^8 \text{ atoms/s} \times P_{\text{Rb87}}(10^{-8} \text{ mbar}).$$

The deviation by a factor 5 of the prediction of the numerical model with respect to the experimental results is due to an overestimation of the radiative force, hence of the capture velocity v_c. Since the number of atoms captured in a VCMOT varies as v_c^4, the capture velocity v_c deduced from our simple model is too high by a factor $(13/2.5)^{1/4} \sim 1.5$. After averaging over the initial direction of the incident atoms, we determine using the numerical simulation $v_c \simeq 32$ m/s. By contrast, the capture velocity in the experimental setup is only $32/1.5 \sim 21$ m/s. In the following graphs 5, 6, 7, we normalize the absolute value of the flux and concentrate on its variation with system parameters.

Simulated VCMOT optimisation

Using the simulation of a pure MOT without push beam, we can readily find the parameters which optimise the capture rate from the background vapour. The total laser power is taken to be 20 mW, equally distributed among three beams which are then retroreflected. We calculate an optimal detuning of -3Γ. The capture rate is reduced by a factor larger than 2 when the detuning is beyond -4.5Γ or smaller than -1.5Γ. The magnetic gradient seems to have little influence as long as it is between 8 and 20 G/cm, which is indeed confirmed in our experimental conditions. In contrast, Lindquist *et al.*, who were using a notably smaller laser power, found a factor 3 decrease in the number of trapped atoms when the gradient varies from 10 to 20 G/cm [10].

It is particularly helpful to use this simulation in order to determine the optimal waist of the trapping beams for a given laser power. A fine tuning of this parameter in the experiment is indeed tiresome since it requires a realignment of the optical setup at each step. In our case, a 9 mm spot size gives the best simulated capture rate, with half
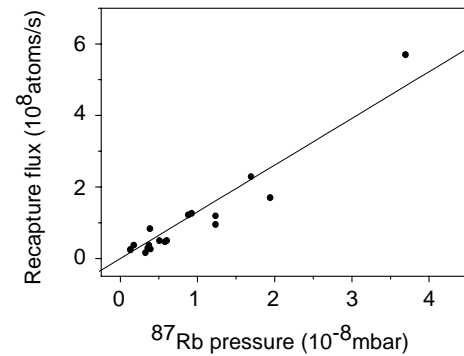

Fig. 4. (●) Experimental measurements of the recaptured flux as a function of the source cell pressure. The linear fit yields $\Phi_{\text{exp}}^{\text{jet}} = (1.3 \pm 0.4) \times 10^8$ atoms/s $\times P_{\text{Rb87}}(10^{-8}$ mbar).

maximum values at 4 mm and 16 mm. This represents the best compromise between a situation with a large capture volume (hence a weak radiation pressure force) and intense laser beams (hence a small trap volume). The optimum parameters do not change significantly if the retroreflection loss of 20% is included in the stimulation.

4.2 The flux of the atom faucet

We now discuss the results obtained when the thin push beam is added to the MOT light field. We first find that the presence of this extra laser beam does not modify the optimal parameters (detuning, intensity, magnetic gradient) of the capture MOT, neither in experiment nor in the simulation. This result is easily understood since the volume affected by the thin push beam (1 mm spot size) is very small compared to the total capture volume defined by the source MOT laser beams (~ 10 mm spot size).

For our optimal experimental parameters for the push beam (see below), the simulation finds 90% transfer from the source MOT through the differential pumping tube to the recapture MOT. The remaining 10% of the atoms leave the source at a divergence too large to be recaptured and are lost. Experimentally, we have achieved a transfer efficiency of $50 \pm 10\%$. This value is most probably limited by the differential pumping tube alignment.

Concerning the total flux, we explored the pressure regime of $10^{-9} < P < 4 \times 10^{-8}$ mbar and found no deviation of the experimental data from a linear dependence (see Fig. 4)

$$\Phi_{\text{exp}}^{\text{jet}} = (1.3 \pm 0.4) \times 10^8 \text{ atoms/s} \times P_{\text{Rb87}}(10^{-8} \text{ mbar}).$$

The uncertainty primarily stems from the determination of the atom number in the recapture MOT by absorption imaging. Deviation from linear scaling with pressure is expected when the collision time with background gas becomes of the order of the typical extraction time from the MOT center into the differential pumping tube. This is the case for $P_{\text{Rb87}} \geq 10^{-7}$ mbar.
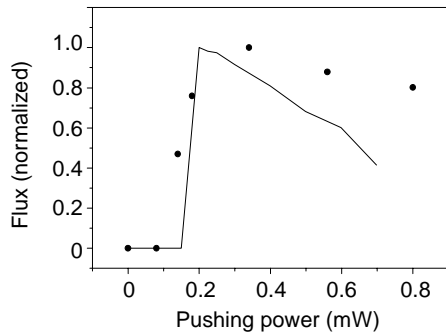
Fig. 5. Dependence of the atomic flux on the push beam power. Flux is normalized, see text. The dots are experimental, the solid line is simulation.

4.3 Push beam parameters

Inspecting qualitatively the calculated trajectories, we find that an atom that enters the volume defined by the intersection of the MOT beams is first decelerated by radiation pressure on a distance much smaller than the trapping beam radius. It then slowly moves to the center of the trap where it enters the extraction column. The final transverse cooling of the jet takes place during extraction, so that the divergence of the jet grows if the extraction happens too fast. This constitutes the key element to understand the influence of push beam power, detuning, and size on the atomic jet emerging from the MOT, that we now discuss in detail.

Power

We find experimentally that for a very low power of the push beam, the trap is decentered but not yet leaking. At $P_{\text{push}} = 80\ \mu$W (corresponding to a push beam intensity 4 times smaller than the intensity of a MOT beam), the flux increases sharply. Then it falls off slowly with increasing power (see Fig. 5).

The simulation predicts the same critical power within experimental errors, without adjustable parameters (see Fig. 5). The decrease at $P > P_{\text{crit}}$ can be understood if one examines the simulated divergence of the atomic jet, which grows with increasing push beam power. This effect is attributed to an insufficiently short transverse cooling time due to the strong acceleration.

The jet velocity is deduced experimentally from measurements like those shown in Figure 2. With increasing push beam power it grows from 12 to 15 m/s with an average width of 10 m/s. In the simulation, we find a much smaller width of 1 m/s. This discrepancy is probably due to the fact that in the simulation we neglected the heating due to spontaneous emission. The measured longitudinal velocity spread is larger than that of the LVIS [6] or 2D MOT [7]; however, for the purpose of loading a recapture MOT, this increase in the longitudinal temperature is not important.
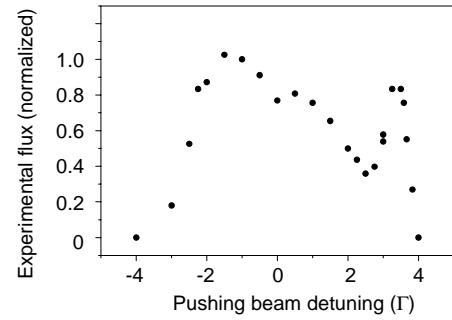

Fig. 6. Dependence of the atomic flux on the push beam detuning. The flux is normalized as indicated in the text.
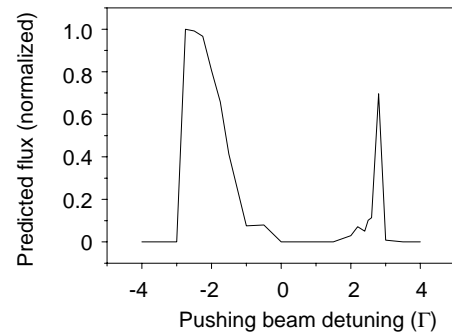

Fig. 7. Simulation of the dependence of the atomic flux on push beam detuning. The flux is normalized as indicated in the text.

Detuning

The complex behaviour of the flux on the push beam detuning (δ_{push}) is qualitatively well reproduced by the simulation (see Figs. 6 and 7).

If the push beam detuning is negative and exceeds the MOT beam detuning ($|\delta_{\text{push}}| > |\delta_{\text{MOT}}|$), the trap is decentered, but not yet leaking. This is easily understood since the intensity of the push beam is about the same as for the MOT beams, so that as the detuning is increased, the radiation pressure force exerted by the push beam becomes weaker than the trapping force.

A negative detuning of the push beam of the same order as the MOT beam detuning corresponds to the optimum situation for the atom faucet. The predictions of the simulation are in full agreement with this clear experimental result.

With zero or small positive detuning, the simulation shows that the atoms are resonantly accelerated, that they leave the source MOT with a large divergence and do not reach the recapture MOT. More precisely, there is a direct correspondence between the divergence of the beam and the extraction time (*i.e.*, flight time from the center of the trap to the depumping region). The physical origin of this correlation is clear: if the extraction acceleration increases, the time available for transverse cooling by the MOT beams decreases, and the transverse velocity spread of the beam is large. Experimentally we find when the

detuning of the push beam approaches 0 that the decrease of the atom flux is less pronounced than what is predicted by our model. This is not fully understood, especially since the experimental results obtained in [18] with a slightly different geometry of the source and recapture MOTs are closer to our theoretical expectations.

For a positive detuning of the push beam such that $\delta_{\text{push}} \simeq |\delta_{\text{MOT}}|$, a prominent peak in the flux appears in both the experiment and the simulation. In order to interpret this result we use the model of a $|g, J_g = 0\rangle \leftrightarrow |e, J_e = 1\rangle$ transition in a one dimensional magneto-optical trap (the actual beam inclination and polarisation make the situation a bit more complicated). For an atom traveling downwards in the extraction column, the $|e, m = -1\rangle$ level approaches the MOT beam resonance at negative detuning. At the same time, the $|e, m = +1\rangle$ level approaches the push beam resonance at positive detuning. When $\delta_{\text{push}} \simeq -\delta_{\text{MOT}}$, the accelerating push beam and the two decelerating upward going MOT beams stay equally close to resonance so that their forces cancel whatever the position of the atom is inside the extraction column. Since there are also downward going MOT beams, the atoms experience a small net downward force and leave slowly. The extraction time is ~ 8 ms and the atoms are cooled transversely leading to a large recapture flux in the lower MOT.

Finally if δ_{push} is positive and larger than $|\delta_{\text{MOT}}|$, the detuning of the $|e, m = -1\rangle$ level from the recentering MOT light is always less than the detuning of the $|e, m = +1\rangle$ level from the push beam light, and so the trap is decentered but not destabilized, in analogy with the behaviour at a large negative detuning.

Complementary numerical study: waist

For a very small push beam radius (< 0.4 mm), we find theoretically that the atoms drift transversely out of the extraction column and decelerate in the longitudinal direction. They can then be recycled or can leave the trap with a large divergence. For a spot size larger than 1.5 mm only a small fraction of the atoms are extracted from the vicinity of the center of the trap, and the remaining ones are not sufficiently transversely cooled to reach the lower trap. Since both cases are less favourable compared to the situation discussed above, we did not investigate them experimentally.

5 Concluding remarks

To summarize, we have presented in this paper an experimental study of an atom faucet, formed by a magneto-optical trap from which a thin laser beam extracts a continuous jet of cold rubidium atoms. We have also presented a 3D simulation of the atomic motion in this multiple laser field configuration. We find that the transverse cooling by the MOT beams *inside* the extraction column turns out to be a crucial element for the satisfactory performance of this leaking MOT atom source. Our simulation overestimates the capture rate of the source upper MOT, but predicts well the measured dependences on the experimental parameters. Moreover, it is readily adapted to an arbitrary laser and B-field configuration.

In comparison with previously demonstrated techniques for transferring cold atoms from a VCMOT into a jet, our atom faucet present clear advantages in terms of flux and/or simplicity for implementation. A moving molasses launch [2] provides a rather cold beam but with low flux. A launch by a resonant push beam from a MOT provides a flux similar to the one obtained in the present work [3,4]. However, during the launch $\sim 1\,000$ photons are scattered by each atom causing a transverse heating. In this case, one may need a magnetic guiding to achieve an elevated transfer efficiency [17], or an extra transverse cooling phase [4].

Continuous schemes suffer less from interparticle interactions than pulsed schemes, since the steady state number of atoms in the MOT remains small. The flux of the beam emerging from a leaking MOT can be comparable with the capture rate of the MOT. The atom faucet presented here provides a transfer efficiency of 50% from first capture in the high pressure MOT to the recapture MOT located in the UHV cell. It creates an extraction column that is typical of leaking MOT systems with a flexible design and without optical parts inside the vacuum chamber. The transfer efficiency compares favorably with the 6% efficiency of the pyramidal funnel [8]. Especially our diverging push beam has no effect on the recapture MOT, in contrast to the light from an MOT beam leaking through a hole in a mirror.

We obtain a flux of $\Phi = 1 \times 10^8$ atoms/s for a background vapour pressure of $P_{\text{Rb87}} = 7.6 \times 10^{-9}$ mbar. This is equal to that of the low power version of the LVIS in [7] and superior to the 2D$^+$ MOT in this pressure region. The later design in turn provides very high flux at high pressure, since it minimizes the source trap density. We could not explore this domain of high pressure in our setup since it was incompatible with the UHV requirements in our recapture cell. However we did not find any deviation from the linear scaling of the flux with pressure up to 4×10^{-8} mbar. Therefore this setup associated with a proper differential vacuum system has the potentiality to produce a flux of several billions of slow atoms per second.

Note added in proofs: After this work was completed, we became aware that a similar setup has been successfully achieved and studied in Napoli, in the group of G. Tino

[18]. A similar device has also been achieved in Innsbruck, in the group of J. Schmiedmayer [19].

References

1. B. Ghaffari, J.M. Gerton, W.L. McAlexander, K.E. Strecker, D.M. Homan, R.G. Hulet, Phys. Rev. A **60**, 3878 (1999).
2. S. Weyers, E. Aucouturier, C. Valentin, N. Dimarcq, Opt. Commun. **143**, 30 (1997).
3. K.I. Lee, J.A. Kim, H.R. Noh, W. Jhe, *Atom Optics SPIE Proc. Series*, Vol. 2995, SPIE, 1997, p. 279.
4. J.J. Arlt, O. Maragó, S. Webster, S. Hopkins, C.J. Foot, Opt. Commun. **157**, 303 (1998).
5. H. Chen, E. Riis, Appl. Phys. B **70**, 665 (2000).
6. Z.T. Lu, K.L. Corwin, M.J. Renn, M.H. Anderson, E.A. Cornell, C.E. Wieman, Phys. Rev. Lett. **77**, 3331 (1996).
7. K. Dieckmann, R.J.C. Spreeuw, M. Weidemüller, J.T.M. Walraven, Phys. Rev. A **58**, 3891 (1998).
8. R.S. Williamson III, P.A. Voytas, R.T. Newell, T. Walker, Opt. Expr. **3**, 111 (1998).
9. K.I. Lee, J.A. Kim, H.R. Noh, W. Jhe, Opt. Lett. **21**, 1177 (1996).
10. K. Lindquist, M. Stephens, C. Wieman, Phys. Rev. A **46**, 4082 (1992).
11. P.D. Lett, W.D. Phillips, S.L. Rolston, C.E. Tanner, R.N. Watts, C.I. Westbrook, J. Opt. Soc. Am. B **6**, 2084 (1989).
12. C.G. Townsend, N.H. Edwards, C.J. Cooper, K.P. Zetie, C.J. Foot, A.M. Steane, P. Szriftgiser, H. Perrin, J. Dalibard, Phys. Rev. A **52**, 1423 (1995).
13. We checked that neither in experiment nor in simulation does the direction of the linear polarization have any effect.
14. C. Cohen-Tannoudji, J. Dupont-Roc, G. Grynberg, *Atom-Photon Interactions, Basic Processes* (Wiley, 1992).
15. F. Reif, *Fundamentals of statistical and thermal physics* (McGraw-Hill, New York, 1965).
16. In order to increase the efficiency of the simulation we only evolve atoms with an initial velocity lower than $v_{\mathrm{max}} = 45$ m/s. We checked that atoms with a larger velocity cannot be captured in the MOT, whatever the direction of their initial velocity.
17. C.J. Myatt, N.R. Newbury, R.W. Ghrist, S. Loutzenhiser, C.E. Wieman, Opt. Lett. **21**, 290 (1995).
18. L. Cacciapuoti, A. Castrillo, M. de Angelis, G.M. Tino, Eur. Phys. J. D **15**, 245 (2001).
19. J. Schmiedmayer, private communication.